Cooperative atomic displacements at sheared twist (001) grain boundaries

2007 J. Phys.: Condens. Matter 19 396005

(http://iopscience.iop.org/0953-8984/19/39/396005)

IOP PUBLISHING JOURNAL OF PHYSICS: CONDENSED MATTER

J. Phys.: Condens. Matter **19** (2007) 396005 (8pp) doi:10.1088/0953-8984/19/39/396005

Cooperative atomic displacements at sheared twist (001) grain boundaries

Francesco Delogu

Dipartimento di Ingegneria Chimica e Materiali, Università degli Studi di Cagliari, piazza d'Armi, I-09123 Cagliari, Italy

E-mail: delogu@dicm.unica.it

Received 23 April 2007, in final form 28 June 2007
Published 3 September 2007
Online at stacks.iop.org/JPhysCM/19/396005

Abstract

Molecular dynamics simulations show that the shear deformation of Cu bicrystals containing a symmetric high-angle twist (001) grain boundary induces the formation of force chains in which a few atoms are pushed against each other. Short-range and relatively long-range atomic displacements take place in the neighborhood of a force chain when its size respectively increases and decreases, promoting the migration of atoms across the grain boundary. The thickness of the layer affected by atomic diffusion processes increases approximately with the square root of time.

(Some figures in this article are in colour only in the electronic version)

1. Introduction

It is well known that internal interfaces like grain boundaries (GBs) to a great extent determine the mechanical, chemical and electrical properties of polycrystalline materials [1]. The influence of GBs on the mechanical behavior is particularly marked in nanocrystalline metals, in which a transition from intragranular to GB-mediated deformation processes is observed as the grain size decreases [2–9]. In the latter regime, plastic deformation is intimately connected with GB mobility. This varies with metallic species and is related to the grain size, the intensity of the applied stresses and the structure of the GB network [1–9]. Depending on such factors, GBs have been shown to either migrate under the effect of thermal and mechanical driving forces or slide against each other [1–11]. When the grain size is smaller than about 15 nm, stress-induced GB sliding can take place even at relatively low temperatures [2, 5, 9, 10]. In this case, individual GB atoms transfer from a given grain to a neighboring one in so-called shuffling events in which point defects are not involved [10, 11]. The description and understanding of such processes is fundamental for achieving a full comprehension and control of the mechanical response of nanostructured metals when no thermally activated mechanism

operates. Despite this, only relatively few studies have investigated the atomistic details of the GB dynamics [12, 13], with the earlier ones mostly focusing on symmetric tilt GBs [10, 12].

In the present work the dynamics of different symmetric twist GBs undergoing shear in a direction parallel to the GB plane is explored by molecular dynamics (MD) simulations.

2. Molecular dynamics simulations

The coincident-site lattice (CSL) [14] high-angle twist GBs $\Sigma 25$ 16.26°, $\Sigma 13$ 22.62°, $\Sigma 17$ 28.07°, $\Sigma 5$ 36.87° and $\Sigma 29$ 43.60° (001) were considered. Calculations were carried out on configurations of Cu atoms arranged in bi-crystals constructed according to the CSL model and the face-centered cubic (fcc) $cF4$ Bravais lattice cell [10, 14]. The bi-crystals investigated had minimum dimensions of about 21, 14 and 14 nm along the x, y and z Cartesian directions respectively, corresponding to about 3.5×10^5 atoms. Periodic boundary conditions were imposed along the x and y Cartesian directions, whereas along the z one bi-crystals were terminated with two reservoir regions [15, 16]. Each reservoir contains eight planes, half of which are immobile. A minimum of 80 mobile (001) planes was used along the z Cartesian direction to minimize the effects of immobile atoms on the GB dynamics and to permit dislocation nucleation and propagation. The number of immobile planes, the farthest ones from the GB, was selected in order that the distance they cover along the z Cartesian direction roughly corresponds to the cutoff radius of the interatomic potential [15, 16]. The latter was described by a semi-empirical many-body tight-binding force scheme based on the second-moment approximation to the electronic density of states [17–19], capable of reproducing the elastic properties of fcc metals with particular accuracy [19]. The potential parameter values were taken from the literature and the interactions were computed within a cutoff radius of about 0.7 nm [19]. Equations of motion were solved with a fifth-order predictor–corrector algorithm [20] and a time step of 2.0 fs. The semi-crystals were separately generated and then approached along the z Cartesian direction up to the distance of minimum enthalpy [16]. The resulting bi-crystals were equilibrated in the isobaric–isothermal *NPT* ensemble at 300 K and null external pressure, with the Nosè–Hoover thermostat and the Parrinello–Rahman scheme implemented over all the mobile species [21–23]. The system dynamics was followed for 6.5 ns. Fluctuations in the potential energy, kinetic energy and volume indicated that the initial configurations relax to equilibrium ones within about 4 ns. The GB position was monitored by calculating the static order parameter $S_p(\boldsymbol{k})$ [20] for the (001) planes of each semi-crystal with suitable reciprocal lattice plane vectors $\boldsymbol{k}$ [16]. No net tendency to migrate was observed either during relaxation or subsequently. The simulation cell is schematically superposed in figure 1 to a relaxed atomic configuration. The corresponding $S_p(\boldsymbol{k})$ profile is also shown.

A normal force along the z Cartesian direction was applied to reservoir atoms at the end of the relaxation stages to produce a small uniaxial stress of about 0.1 MPa. The distance between reservoirs was thus kept roughly constant with no rigid constraint, facilitating the accommodation of atomic strains [15, 24]. Shearing was simulated by applying a force to reservoirs along the x Cartesian direction [15, 24]. The force intensity was selected in order to produce a relative sliding velocity u_p of about 10 m s^{-1}, a relatively small value which still allows the induction of shear deformation in times accessible for computations [15, 24]. Such a value should be quite close to the minimum threshold below which sliding becomes irregular and inhomogeneous, preventing the formation of a well-defined sliding pair [15, 24]. The threshold value, in turn, strongly depends on the number of mobile planes between the two reservoir regions as well as on the extension of the interfacial area shared by sliding pairs [15]. A velocity field with linear profile in the range between $-u_p/2$ and $+u_p/2$ was imposed for 2 ps to the atomic planes outside reservoirs to avoid shock waves [15, 24]. Strain rates were

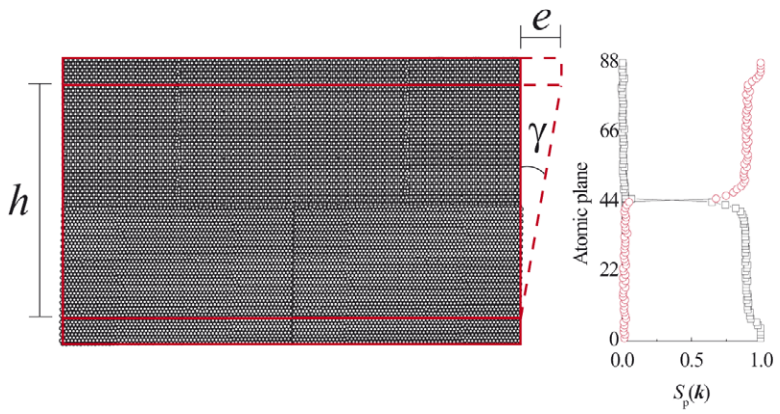

Figure 1. Projection on the $(x–z)$ Cartesian plane of the relaxed atomic configuration for a $\Sigma 13$ 22.62° (001) high-angle twist GB. Immobile reservoir atoms as well as GB ones are shown in dark gray. The simulation cell is schematically superposed to show reservoir regions at distance h and deformation effects, which produce an average shear displacement e and thus a shear strain $\gamma = \arctan(e/h)$. The profiles of $S_p(\boldsymbol{k})$ for each semi-crystal (001) planes are also shown.

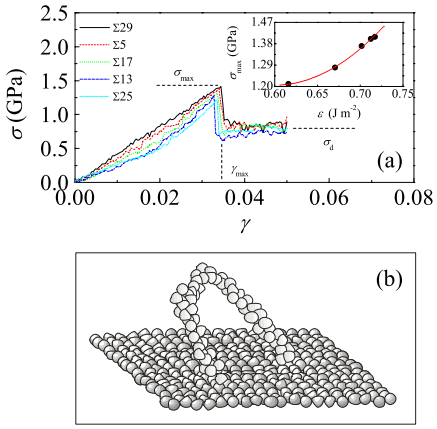

Figure 2. (a) The average stress σ as a function of the average strain γ for the GBs investigated. The average stress drops from the maximum value $\sigma_{\max}$ attained at the average strain $\gamma_{\max}$ to a smaller value σ_d, roughly equal for all the systems. The inset shows that $\sigma_{\max}$ increases with the GB energy ε according to a quadratic trend. (b) A partial dislocation at the $\Sigma 25$ GB after about 110 ps. Light gray atoms have centrosymmetry parameter P values between 0.39 and 3.14 Å^2.

on the order of 6×10^8 s^{-1}. Time t was scaled to 0 at the beginning of shearing. During shearing, only mobile reservoir atoms were thermostatted to permit a spontaneous kinetic energy distribution.

3. Results and discussion

Mechanical responses of twist GBs to shear are reported in figure 2(a), where the average stress σ is quoted as a function of the average strain $\gamma = \arctan(e/h)$. Here e and h are respectively the shear displacement and the distance between reservoirs [25]. The average stress was instead

estimated by evaluating the local stress tensor for each atom and then averaging over all the mobile species [25]. Bi-crystals exhibit similar curves. A roughly linear increase of σ with γ is observed in the initial elastic deformation regime, replaced by the plastic one when the average stress drops from the maximum value σ_{max} attained at the average strain γ_{max} to a smaller value σ_d. The average strain γ_{max} required for obtaining plastic deformation decreases as the GB angle increases, and a quadratic relationship between yield stress σ_{max} and GB energy ε is found, as shown in the inset of figure 2(a). All the systems tend to attain approximately the same plateau σ_d value. The abrupt stress relaxation is associated with the nucleation of dislocations, which accompany the onset of the sliding behavior at GBs. The atomic species involved in line defects were identified according to their centrosymmetry parameter P values [26], which quantify the degree of structural order within the coordination shell. More specifically, the centrosymmetry parameter P exploits the fact that in centrosymmetric lattices such as the fcc one each atom has pairs of equal and opposite 'bonds' to its nearest neighbors [26]. When a lattice distortion is introduced both the direction and length of these bonds could change, but the bonds would remain equal and opposite [26]. In contrast, when atoms are involved in or interact with a defect such a relationship no longer holds true for all the nearest-neighbor pairs [26]. It follows that P allows one to distinguish plastic deformation from elastic deformation. In addition, systematic studies have also shown that a characteristic range of P values pertains to atoms involved in given defective configurations [26]. In accordance with the literature [26], the atoms involved in partial dislocations display P values roughly between 0.39 and 3.14 Å^2. GB atoms have, instead, P values on the order of 10 Å^2.

Dislocations nucleate from GBs. Here the species have larger atomic volumes Ω, quantified via the classical Voronoi's polyhedra space tessellation [27, 28], which favor their rearrangement and the accommodation of atomic strains in the planes adjacent to GBs. Slip occurs mostly on the $(111)[\bar{1}01]$ and $(11\bar{1})[101]$ slip systems and it initially causes the appearance of partial dislocations, shown in figure 2(b). As deformation proceeds, the partial dislocations progressively move away from the GB, leaving behind intrinsic stacking faults. Small dislocation loops are also emitted.

The formation and propagation of dislocations are triggered by the localization of shear events. During such events atoms are compressed each against the other and they approach distances significantly shorter than the ones attained during thermal vibrations, thus experiencing strong repulsive interactions. Thermal vibration and local shear stress effects were discriminated by using a threshold distance criterion. The threshold distance r_t was defined as $r_0 - 3\sigma$, where r_0 corresponds to the position of the first peak of the pair correlation function (PCF) [20] and σ to the mean-square deviation of the Gaussian best fitting the peak. Atoms located at distances shorter than r_t form connected clusters, hereafter referred to as force chains (FCs) [29]. The aforementioned distance criterion was used to evaluate the total number N_{fc} of FCs and their size n_{fc}, i.e. the number of atoms connected in each FC [29]. The approximate fractal dimension d_{fc} of each FC was estimated by relating n_{fc} to L_{fc}, which is the maximum distance between atoms in the same FC [30].

The behavior of n_{fc} as a function of time t reveals that an FC is a quickly evolving entity. Figure 3 shows that n_{fc} increases irregularly up to a maximum and then rapidly decreases. The decrease can be so pronounced that n_{fc} attains a null value and the FC disappears. Alternatively, the FC can survive up to a successive n_{fc} increase and then disappear, as shown in figure 3. The maximum number of cycles of increase and decrease observed for a given FC is three. The inset in figure 3 shows that during the n_{fc} increase stage the FC fractal dimension d_{fc} increases from about 1 to roughly 1.6. The latter value highlights the ramified stringy structure of FCs at their maximum size, somewhat similar to that of random walks [30]. The total number N_{fc} of FCs remains, instead, at a roughly constant value of 20.

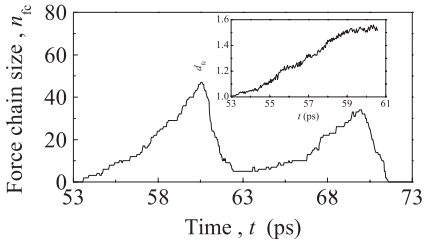

Figure 3. The FC size n_{fc} as a function of time t for the bi-crystal containing a $\Sigma 5$ GB. The inset reports the FC fractal dimension d_{fc} as a function of time t for the first n_{fc} increase stage quoted in the figure.

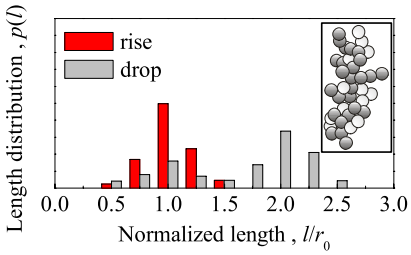

Figure 4. Normalized distributions $p(l)$ of atomic displacements of length l during the time intervals of n_{fc} rises and drops. An FC is shown in the inset together with (light gray) atoms with volume $\Omega > 1.1\Omega_{av}$, Ω_{av} being the average volume. Data pertain to the bi-crystal containing a $\Sigma 29$ GB.

Different atomistic processes operate during n_{fc} rises and drops, although always originated from the attempt of atomic species of accommodating local strains. In the former stage, the localization of mechanical forces promotes the occurrence of short-range atomic displacements restricted to the coordination shell. Such displacements typically involve two atoms neighboring the FCs and result in their position exchange. The process is related to the production of excess free volume in the neighborhood of FCs. The compressive forces operating during local shear events are indeed sustained by FCs, so such compressive forces do not directly involve atoms neighboring the FCs. These species, shown in the inset of figure 4, experience instead a sort of decompression and have atomic volumes Ω significantly larger than the average Ω_{av}. This facilitates atomic rearrangements even though no point defect can actually be identified. In the n_{fc} drop case, the FCs are no longer able to withstand the mechanical forces, and partial dislocations form and propagate via a fast rearrangement of atomic species. Such rearrangement is accompanied by a redistribution of the excess volume and can result in atomic displacements on distances up to $3r_0$.

It is worth noting here that drops in FC size n_{fc} and emission of partial dislocations are intertwined processes. Partial dislocations always appear in the same region of space previously occupied by atoms involved in FCs. Although a fully satisfactory characterization of the relationship between the two aforementioned processes has not been possible due to the relatively large size of FCs and the consequent undefined volume occupied by FCs, it seems possible to regard FCs as precursors to the nucleation of dislocations. It should also be noted that additional simulations carried out on the system containing the $\Sigma 29$ GB under the same previously specified conditions but with sliding velocity u_p in the range between 20 and 40 m s^{-1} have shown that the rate of FC appearance and disappearance, as well as of

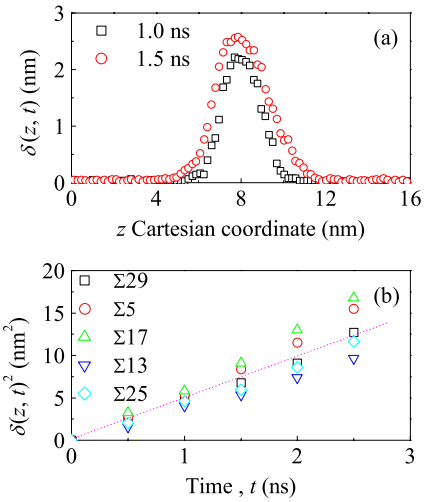

Figure 5. (a) The $\delta(z, t)$ values along the z Cartesian direction for a bi-crystal containing a Σ29 GB at the times indicated. Data are fitted with Gaussians centered at z_0. (b) The roughly linear scaling of $\delta(z_0, t)^2$ with time t for the GBs investigated. The dotted line is a guide for the eyes.

dislocation nucleation processes, is dependent on the strain rate. However, this does not affect their fundamental features, and the relationship between the processes is further confirmed.

The difference between atomic rearrangement processes during n_{fc} rises and drops can be revealed by examining the distribution $p(l)$ of atomic displacements of length l during the time intervals over which rises and drops occur. Distributions are calculated for each FC within the region defined by a distance of $3r_0$ from each FC atom and then mediated over all the FCs. Results are reported in figure 4. A narrow distribution peaked at about r_0 pertains to the stage of n_{fc} increase, whereas the distribution of displacements during the n_{fc} decrease is significantly broader, being bimodal with maxima roughly at r_0 and $2r_0$.

Atomic displacement processes taking place during n_{fc} rise and drop stages must be regarded as cooperative shuffling events in which the redistribution of atomic volume is associated with the coordinated motion of 2 to roughly 10 atoms. Their occurrence promotes the exchange of atoms between the semi-crystals. It is worth noting here that in no case were dislocations crossing GBs observed. Single dislocations are always located in a given half of the semi-crystal and they do not cross the GB region to propagate into the opposite half. Unlike dislocations, FCs extend instead across GBs, so each FC includes atomic species belonging to both semi-crystals. Atomic mixing was quantitatively monitored by evaluating the mixing parameter $\delta(z, t)$ [31], which measures the total amount of displacement along the z Cartesian direction within a layer of thickness dz respect to the fraction of displacement due to the possible shift of the center of mass of such layer [31]. The larger the $\delta(z, t)$ value, the further the atoms move from their original positions. As shown in figure 5(a), $\delta(z, t)$ can be fitted reasonably well with a Gaussian centered at z_0, which corresponds to the GB position along the z Cartesian direction. This clearly indicates that atomic displacements mostly occur in the GB region, where atomic species possess on average larger atomic volumes Ω.

It follows that atomic mixing processes mostly occur in the same region. A layer of mixed species thus grows at the GBs. A measure of its thickness is given by $\delta(z_0, t)$ [31], which represents the time-dependent breadth of the Gaussian centered at z_0 fitting the distribution of atomic displacement. Numerical findings reveal that the mixed layer thickness $\delta(z_0, t)$

increases with time t. The data obtained for the different GBs investigated are shown in figure 5(b), where $\delta(z_0, t)^2$ is quoted as a function of t. It can be seen that in all cases the data followed a remarkably linear trend.

It should be noted that the roughly linear scaling observed suggests that the thickness of the mixed layer $\delta(z_0, t)$ has a kinetic dependence on time t, analogous to that generally observed when a thermal diffusion mechanism operates [31]. In this case, however, atomic displacements are not mediated by single vacancies diffusing on regular lattice sites. On the contrary, relatively short-range and long-range displacements originate from cooperative rearrangements of atomic species in strained configurations.

4. Conclusions

Numerical findings reveal that the shear-induced sliding of high-angle twist GBs is controlled by a complex sequence of atomistic processes. It appears that during the course of elastic deformation shear stresses localize in a few areas of the GB region. Such localization can be suitably followed by monitoring the formation of FCs across GBs in which atoms interact with relatively strong repulsive forces. The FCs undergo stages of size increase and decrease with different and characteristic consequences for atomic displacements. In particular, the fast size decrease or disappearance of FCs is related to the onset of local plastic deformation events, i.e. to the emission of partial dislocations. The sudden rearrangement of atoms when dislocations nucleate and propagate is responsible for the exchange of atoms between the two halves of the semi-crystals, which always remain well distinguished. Atomic mixing is particularly pronounced at GB regions, where atoms possess excess free volume, and diminishes gradually with distance from the GBs. Interestingly, the thickness of the layer involved in mixing processes displays a dependence on time analogous to that of thermal diffusion. This poses intriguing questions concerning the stochastic character of shear-induced atomic displacement events which deserve further attention.

Acknowledgments

A Ermini, ExtraInformatica s.r.l., is gratefully acknowledged for technical support. Financial support was given by the University of Cagliari.

References

[1] Wolf D and Yip S (ed) 1992 *Materials Interfaces* (London: Chapman and Hall)
[2] Schiotz J *et al* 1998 *Nature* **391** 561
[3] Liao X Z *et al* 2003 *Appl. Phys. Lett.* **83** 632
[4] Chen M *et al* 2003 *Science* **300** 1275
[5] Schiotz J and Jacobsen K W 2003 *Science* **301** 1357
[6] Kumar K S *et al* 2003 *Acta Mater.* **51** 5743
[7] Yamakov V *et al* 2004 *Nat. Mater.* **3** 43
[8] Van Swygenhoven H *et al* 2004 *Nat. Mater.* **3** 399
[9] Lund A C *et al* 2004 *Phys. Rev.* B **69** 012101
[10] Sansoz F and Molinari J F 2005 *Acta Mater.* **53** 1931
[11] Van Swygenhoven H and Derlet P M 2001 *Phys. Rev.* B **64** 224105
[12] Rittner J D and Seidman D N 1996 *Phys. Rev.* B **54** 6999
[13] Zhang H *et al* 2006 *Phys. Rev.* B **74** 115404
[14] Schonfelder B 2003 *PhD Thesis* RWTH Aachen
[15] Hammerberg J E *et al* 1998 *Physica* D **123** 330
[16] Lutsko J F *et al* 1989 *Phys. Rev.* B **40** 2841

[17] Ducastelle F 1970 *J. Physique* **31** 1055
[18] Rosato V *et al* 1989 *Phil. Mag.* A **59** 321
[19] Cleri F and Rosato V 1993 *Phys. Rev.* B **48** 22
[20] Allen M P and Tildesley D 1987 *Computer Simulation of Liquids* (Oxford: Clarendon)
[21] Andersen H C 1980 *J. Chem. Phys.* **72** 2384
[22] Nosè S 1984 *J. Chem. Phys.* **81** 511
[23] Parrinello M and Rahman A 1981 *J. Appl. Phys.* **52** 7182
[24] Delogu F and Cocco G 2005 *Phys. Rev.* B **72** 014124
[25] Horstemeyer M F *et al* 2001 *Theor. Appl. Fract. Mech.* **37** 49
[26] Kelchner C L *et al* 1998 *Phys. Rev.* B **58** 11085
[27] Voronoi G F 1908 *J. Reine Angew. Math.* **134** 198
[28] Finney J L 1970 *Proc. R. Soc.* A **319** 495
[29] Delogu F and Cocco G 2006 *Phys. Rev.* B **74** 035406
[30] Braunstein L A *et al* 2002 *Phys. Rev.* E **65** 056128
[31] Fu X Y *et al* 2001 *Wear* **250** 420